From Hamiltonian perturbation theory to symplectic integrators and back

Giancarlo Benettin [1] and Francesco Fassò [2]

Università di Padova, Dipartimento di Matematica Pura e Applicata, Via G. Belzoni 7, 35131 Padova, Italy.
E-mail: benettin,fasso@math.unipd.it

Hamiltonian perturbation theory explains how symplectic integrators work and, in particular, why they can be used to measure extremely small energy exchanges between different degrees of freedom in molecular collision problems. Conversely, numerical experiments based on symplectic integrators permit a detailed understanding of the dynamics of nearly integrable Hamiltonian systems, thus providing a valuable support to Hamiltonian perturbation theory.

1 Introduction

Symplectic integrators are well-known to give good results for Hamiltonian systems. Especially good results are obtained for scattering problems; i.e., when, asymptotically, for $t \to \pm\infty$, the algorithm becomes exact. In particular, for molecular collision problems, symplectic integration permits us to measure extremely small energy exchanges between different degrees of freedom. On the one hand, Hamiltonian perturbation theory allows us to understand how symplectic integrators work, and explains why the precision is so high for scattering. On the other hand, the possibility of making accurate numerical experiments using symplectic integrators helps us understand in detail the dynamics of nearly integrable Hamiltonian systems, thus providing a valuable support to Hamiltonian perturbation theory.

The purpose of this paper is to review critically in this perspective the relationship between perturbation theory and symplectic integration. We start from a well defined physical problem, briefly illustrated in Section 2; to show

[1] Istituto Nazionale di Fisica della Materia and Gruppo Nazionale di Fisica Matematica (CNR)
[2] Gruppo Nazionale di Fisica Matematica (CNR)

Preprint submitted to Elsevier Preprint *3 June 1998*

how powerful symplectic integration can be, we study it (far beyond the domain of physical interest!) by means of multiprecision computations. Section 3 is devoted to understanding symplectic integration within Hamiltonian perturbation theory, and Section 4 to the contributions symplectic integration can provide to the further development of the theory.

2 The physical problem, and multiprecision numerical results

At the turn of the century, Boltzmann [8,9] and Jeans [11] suggested that the energy exchanges due to molecular collisions between the translational and vibrational (or rotational) degrees of freedom in classical gases are extremely small if the frequency of vibration (or rotation) is sufficiently high. Their goal was to understand why the fast internal degrees of freedom of the molecules, in ordinary conditions, are hardly involved in energy sharing (they are "frozen", in the later quantum language) and so do not contribute to the thermodynamics of the system. Fig. 1 illustrates a few very elementary models for molecular collisions. Models (a) and (b) represent the collision of a purely vibrating or a purely rotating molecule against a wall and are very similar since both include a single high frequency. If the molecules are identical, model (c) also has a single frequency and is not essentially different from the previous models. In contrast, model (d) has two independent frequencies; as we shall see, this leads to relevant differences. More complicated collision processes could be considered, but we shall not discuss them here.

Jeans in particular understood, on the basis of heuristic considerations, that in models with a single frequency the energy exchange ΔE, averaged over the phase ϕ of the fast internal degree of freedom, should decrease exponentially with the frequency; i.e., with $\langle\,\cdot\,\rangle_\phi$ denoting averaging on ϕ,

$$\langle \Delta E \rangle_\phi \simeq \mathcal{E}_0\, e^{-\tau_0 \omega} \ , \tag{1}$$

for suitable $\mathcal{E}_0$, $\tau_0 > 0$. A similar conclusion was reached later by Landau and Teller [12] (see also [16]), for the apparently different, but in fact intimately related, problem of dispersion of sound waves in diatomic gases.

The approximation introduced by Landau and Teller, known among physicists as "computation along unperturbed orbits" is revisited and adapted to the Boltzmann–Jeans problem in [5]. Here we use the conclusions, and to be definite we make reference to the simple case of a rotator which collides with a potential well (Fig. 1b). The Hamiltonian is

$$H(p, I, x, \phi) = \frac{I^2}{2A} + \frac{p^2}{2m} + V(x, \phi) \ , \tag{2}$$

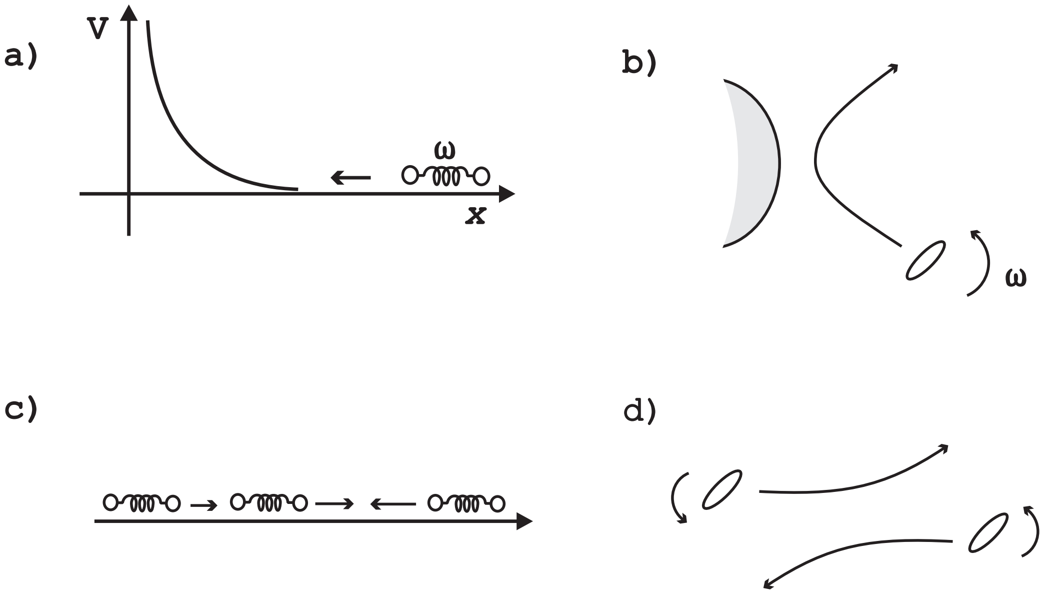

Fig. 1. Elementary examples of collision processes.

where A, m, I and p are, respectively, the moment of inertia, the mass, the angular momentum and the linear momentum of the rotator. Concerning V, the only important requirement is that it is analytic and it describes a collision process, say it has the form of a (smooth) barrier near $x = 0$, and it vanishes at infinity. We shall here consider

$$V(x, \phi) = U(x + a\cos\phi) \ , \qquad U(r) = U_0 e^{-r^2}/r \ , \tag{3}$$

where a is a small constant, but different choices of V lead to similar results. Let p^o, I^o, ϕ^o be the asymptotic data, defined by the limits

$$\begin{array}{ll} p(t) \to -p^o & x(t) + \dfrac{p^o}{m} t \to 0 \\ I(t) \to \ I^o & \phi(t) - \omega t \to \phi^o \ , \end{array} \tag{4}$$

as $t \to -\infty$, where $\omega = I^o/A$. The result of the Landau–Teller approximation, expected to be good for large ω, is

$$\Delta E(\omega, p^o, \phi^o) = \sum_{k \in \mathbf{Z}} E_k(\omega, p^o)\, e^{ik\phi^o} \ , \tag{5}$$

with E_k exponentially small in ω, namely

$$E_k = \mathcal{E}_k\, e^{-|k|\tau\omega} \qquad \text{for} \quad k \neq 0 \ , \qquad E_0 = \mathcal{E}_0\, e^{-2\tau\omega} \ . \tag{6}$$

Here the crucial quantity τ, depending on p^o, is the width of the analyticity strip of the solution of the unperturbed Hamiltonian system

$$\mathcal{H}(p,x) = \frac{p^2}{2m} + \langle V \rangle_\phi(x), \tag{7}$$

corresponding to the asymptotic condition $p(-\infty) = -p^o$, considered as a function of the complex time t; the coefficients $\mathcal{E}_k$ depend on p^o and also on ω, but much less than exponentially. The approximation is in agreement with (1) when $\tau_0 = 2\tau$.

This heuristic result gives strong support to the ideas of Boltzmann and Jeans. But is it reliable? No control is provided by the theory on the possible higher order corrections which, in principle, could even invalidate the exponential law (see [2,4]). In this situation, numerical integration can provide a useful check. Quite clearly, to check the exponential laws, we should be able to measure *very* small energy exchanges (and to separate Fourier components with very different amplitudes; see (6)). Here, as we shall see, symplectic integration schemes exhibit an outstanding superiority with respect to other apparently more accurate formulas.

In [1,5,18], using a symplectic integrator, namely the so–called leapfrog, and quadruple precision (33 decimal figures), it was possible to measure energy exchanges as small as 10^{-30} (in natural units), and to check the validity of the Landau–Teller approximation up to this limit.[3] However, this lower limit is not intrinsic to the theory; rather, it is due to round-off and moves to smaller values in multi-precision arithmetics. We repeated the numerical experiments using higher precision arithmetics (up to 109 digits), and the results, E_k versus ω for $k = 0, 1, 2, 3$, are reported in Fig. 2, for $m = 1$, $A = 1$, $a = 10^{-1}$ and $p^o = \sqrt{2}$. Clearly, the numerical data follow the exponential laws (6) up to energy exchanges smaller than 10^{-90}. As is also remarkable, it is possible to separate the Fourier components even when the ratio between their coefficients is as large as, say, 10^{-60} (see Appendix A). The algorithm was leapfrog with time step $\varepsilon = 0.013\,(2\pi/\omega)$.

A spontaneous comment in front of these results is that they are impossible. Indeed, the errors in energy conservation, during the collision, are *much* larger than the quantity ΔE which we claim to measure, so the results seem meaningless. However, the question is more subtle. As first observed in [1], the relative error in energy conservation,

$$\delta E(t) = \frac{E(t) - E(-\infty)}{E(-\infty)} \ , \tag{8}$$

[3] These results include different choices of the interaction potential and different models, including oscillators; see Fig. 1a, c.

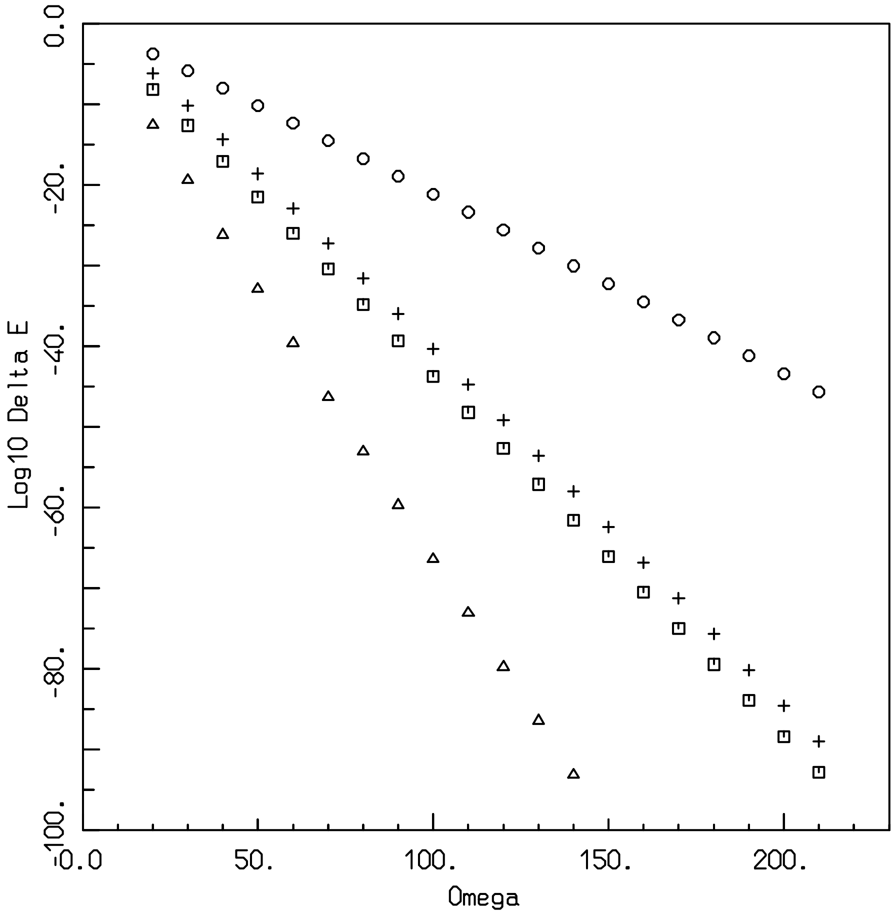

Fig. 2. E_k vs. ω, for $k = 1, 2, 0, 3$ (top to bottom).

is fairly large during the collision, but reduces and nearly vanishes after the collision; see Fig. 3. More specifically, during the collision, the error δE scales [4] as ε^2, as expected with leapfrog, while at the end of the collision it decreases exponentially with $1/\varepsilon$, and is soon as small as 10^{-100}; see Fig. 4. This behavior is characteristic of symplectic integrators, and is lost when using non-symplectic integrators (see Appendix B for a comparison with Runge-Kutta).

3 From Hamiltonian perturbation theory to symplectic integrators...

Consider a generic Hamiltonian $H(p, q)$, $(p, q) \in \mathbf{R}^{2n}$ and let Φ_t^H be its flow. A symplectic integrator of order s is nothing else than a symplectic map Ψ_ε,

[4] Specifically, under the conditions of Fig. 3, if ε is reduced by a factor 10, the highest peak reduces by a factor 100.006.

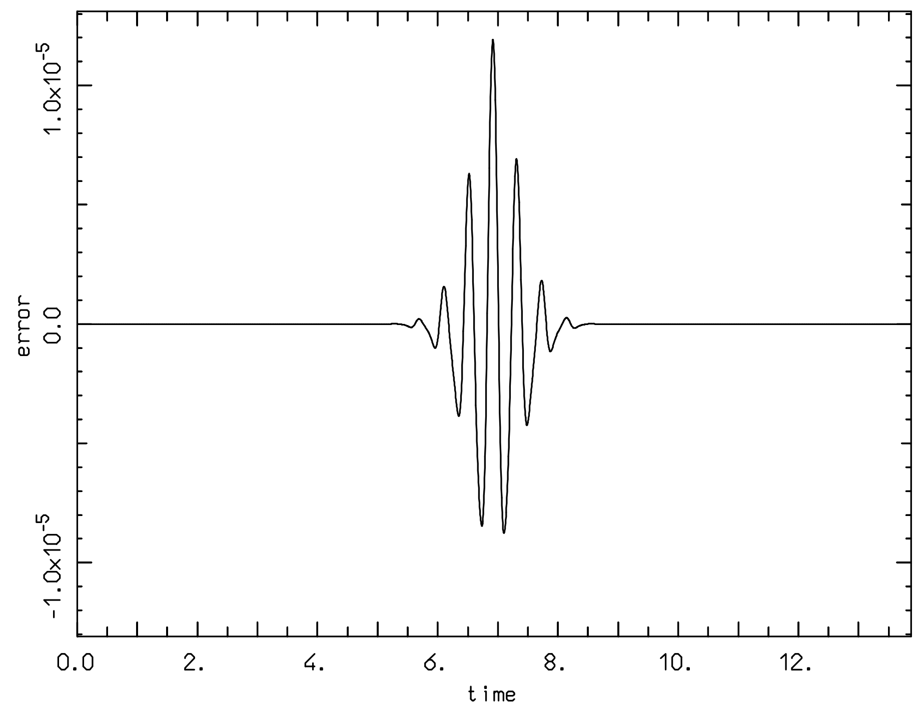

Fig. 3. The relative error in energy conservation as function of time, for $\omega = 15$, $m = 1$, $A = 1$, $a = 0.1$, $p^o = 2^{1/2}$, $\varepsilon = 0.005\frac{2\pi}{\omega}$.

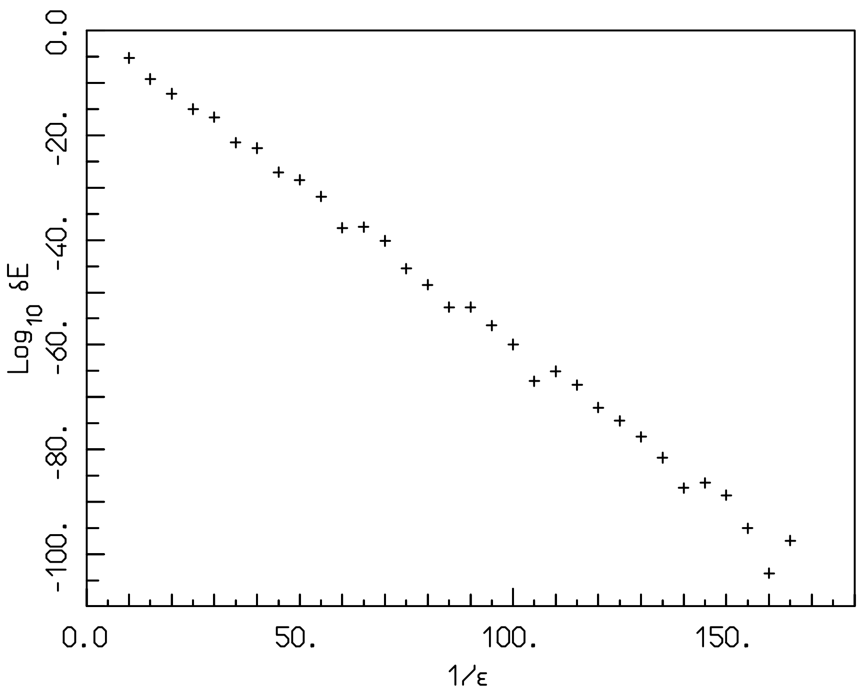

Fig. 4. The final value of δE vs. $1/\varepsilon$, same conditions as Fig. 3.

ε-close to the identity, such that

$$\Psi_\varepsilon - \Phi_\varepsilon^H = \mathcal{O}(\varepsilon^{s+1}) \ . \tag{9}$$

As discussed for example in [7,10,13–15,17], perturbation theory provides a useful framework for understanding the behavior of symplectic integrators. In essence, if Ψ_ε is analytic and admits a global generating function, there exists a "nearly interpolating" Hamiltonian K_ε such that

$$\Psi_\varepsilon - \Phi_\varepsilon^{K_\varepsilon} = \mathcal{O}(\varepsilon\, e^{-1/\varepsilon}) \ ; \tag{10}$$

moreover, K_ε is near to H, namely

$$K_\varepsilon - H = \mathcal{O}(\varepsilon^s) \ . \tag{11}$$

Such a result has several consequences, including the fact that the error in energy conservation is bounded nearly uniformly in time:

$$H \circ \Psi_\varepsilon^k - H = \mathcal{O}(\varepsilon^s) \qquad \text{for} \quad k \sim \varepsilon^{1-s}\, e^{1/\varepsilon} \ . \tag{12}$$

Fig. 5a symbolically illustrates the situation: the solid and dashed lines represent the surfaces $H = E$ and $K_\varepsilon = E$, respectively; one moves near the latter (for an exponentially long time), and the apparent error δE is nothing else than the relative oscillation of the surfaces. As a matter of fact, what one really does in the numerical study of a Hamiltonian system by means of a symplectic integrators, is replacing the original Hamiltonian H by a nearby K_ε, and then computing with essentially no error (but for round-off, as with maps). Of course, if small changes in H are expected to change the properties of the system essentially, then numerical results (independently of the accuracy and of the integration method, in our opinion) are meaningless. Instead, if the properties of interest are "robust" and are expected to persist under small perturbations, then numerical results are reliable, and in particular δE should not be regarded as an effect of numerical errors, rather as due to a lack of knowledge of the details of the system.

All of these considerations are for general Hamiltonians $H(p,q)$ and are insufficient to explain the case of scattering, in particular the behavior of δE in Figs. 3 and 4. Scattering is discussed in detail in [7]; here, we make explicit reference to the Hamiltonian (2) with V as in (3). In this case, leapfrog is the map $(x,\phi,p,I) \mapsto (x',\phi',p',I')$ given by

$$x' = \quad x + \varepsilon \frac{p}{m} \ , \qquad\qquad \phi' = \phi + \varepsilon \frac{I}{A} \ ,$$

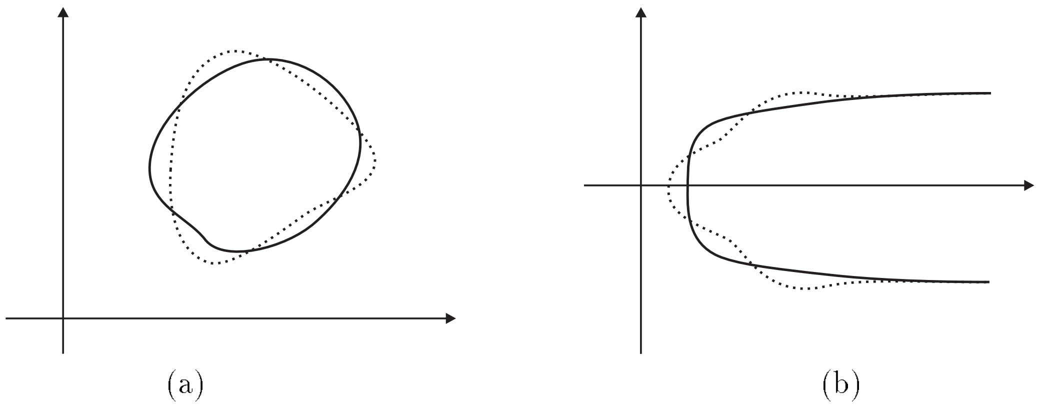

Fig. 5. Energy conservation with symplectic integrators (a) the general case and (b) the case of scattering; solid line: surface $H = E$, dashed line: surface $K_\varepsilon = E$.

$$p' = p - \varepsilon \frac{\partial V}{\partial x}(x', \phi') \ , \qquad I' = I - \varepsilon \frac{\partial V}{\partial \phi}(x', \phi') \ , \tag{13}$$

and, as is crucial, the algorithm becomes exact when, for $x \to \infty$, V and its derivatives vanish. More precisely, there exists a function $\mathcal{V}$ which, for large x, vanishes essentially as V, that is, in our example as e^{-x^2}, such that (9) and (10) may be replaced by local inequalities of the form

$$\begin{aligned} &|\Psi_\varepsilon(z) - \Phi_\varepsilon^H(z)| < c_1 \, \varepsilon^2 \, \mathcal{V}(x), \\ &|\Psi_\varepsilon(z) - \Phi_\varepsilon^{K_\varepsilon}(z)| < c_2 \, \varepsilon \, e^{-\varepsilon^*/\varepsilon} \, \mathcal{V}(x) \ , \end{aligned} \tag{14}$$

where $z = (p, I, x, \phi)$ and c_1, c_2, ε^* are constants. The immediate consequence is that K_ε is preserved exponentially well, uniformly in time:

$$|K_\varepsilon(\Psi_\varepsilon^k(z)) - K_\varepsilon(z)| < c_3 \varepsilon \, e^{-\varepsilon^*/\varepsilon} \ . \tag{15}$$

Furthermore, the true and interpolating Hamiltonians H and K_ε coincide for large x, specifically,

$$|K_\varepsilon(z) - H_\varepsilon(z)| < c_4 \, \varepsilon \, \mathcal{V}(x) \ , \tag{16}$$

and the corresponding surfaces of constant energy glue at infinity (in both directions) as illustrated symbolically in Fig. 5b. The regular oscillations of δE in Fig. 3 are nothing but the relative oscillations of the two energy surfaces; thanks to the glueing, the oscillations vanish at infinity.

As in the general case, for scattering it is inappropriate to say that there are errors in E, rather that the Hamiltonian one is actually studying, namely K_ε, does not coincide exactly with H. But, there are no reasons to prefer one Hamiltonian over the other: unfortunately, both are quite different from realistic Hamiltonians, and in fact, all interest in the Boltzmann–Jeans problem is due to the fact that the details of the system at hand are not believed to be relevant.

All of this, let us stress, can be put in a precise mathematical form, and is covered by theorems which are stated and proven within Hamiltonian perturbation theory. This is, so to speak, the contribution of perturbation theory to symplectic integration.

4 ... and back to perturbation theory

Once we are confident in the numerical results from symplectic integration, in particular in scattering problems, they can be used as valid support for developing perturbation theory. Indeed, numerical investigations arrive where rigorous theory does not, and can provide answers to open questions, checks of conjectures, and hints for further theoretical developments.

The above check of the Landau–Teller approximation, which was our main motivation to become interested in symplectic integrators, is already a good example in this direction. Indeed it is possible, and not difficult, to study analytically Hamiltonians like (2) by the usual instruments of classical perturbation theory [6], and provide rigorous bounds to the energy exchange ΔE, of the form

$$|\Delta E| < E^* e^{-\omega/\omega^*} \ . \tag{17}$$

However, such estimates, although obviously interesting because rigorous, are rather poor for several reasons: (i) they provide only upper bounds on ΔE (useful to deduce only lower bounds on the equilibrium times in gases); (ii) the constants E^* and ω^* are overestimated and unrealistic; and (iii) the different behavior of different Fourier components [5] is lost. More detailed results, essentially a rigorous version of the Landau–Teller approximation, can be obtained perturbatively for special systems [4], but physically interesting conclusions are beyond current perturbation theory; even for the simple case of systems with a single frequency, numerical studies continue to play a significant role.

A more interesting situation is given by systems with two or more frequencies.

[5] For the approach to statistical equilibrium in gases, it is crucial to distinguish between the maximum and average energy exchange (Fourier components with $|k| \geq 2$ are instead irrelevant).

The simplest example (similar to the collision problem in Fig. 1d) is perhaps the case of two rotators coupled by a time–dependent analytic potential which vanishes for $|t| \to \infty$ [3]. The Hamiltonian is

$$H(I_1, I_2, \phi_1, \phi_2) = \frac{I_1^2}{2} + \frac{I_2^2}{2} + f(t)\, g(\phi_1, \phi_2) \ , \tag{18}$$

with

$$f(t) = \frac{e^{-t^2}}{\tau^2 + t^2} \ , \qquad\qquad g(\phi) = \frac{1}{2} \sum_{k \in \mathbf{Z}^2} e^{-\rho|k|} e^{ik\cdot\phi} \ , \tag{19}$$

where $|k| = |k_1| + |k_2|$, I_1 and I_2 are the angular momenta of the rotators, and ρ and τ are positive constants. Denote by $\omega = (\omega_1, \omega_2)$, $\omega_i = I_i(-\infty)$, the asymptotic angular velocity, and consider the case of large ω, more precisely,

$$\omega = \lambda\, \Omega, \tag{20}$$

with fixed $\Omega \in \mathbf{R}^2$ and large λ. Our concern is with the accuracy of conservation of I_1 and I_2, which are adiabatic invariants; i.e., with

$$\Delta I = (\Delta I_1, \Delta I_2) \ , \qquad \Delta I_j = (I_j(+\infty) - I_j(-\infty)) \ , \qquad j = 1, 2 \ . \tag{21}$$

The arithmetic properties of $x = \Omega_2/\Omega_1$ are crucial (so Ω is kept fixed); we restrict attention to the simple case $x = \sqrt{2}$. The continued fraction expansion $\sqrt{2} = [1; 2, 2, 2, \ldots]$, gives the sequence of best rational approximants,

$$\frac{3}{2}, \ \frac{7}{5}, \ \frac{17}{12}, \ \frac{41}{29}, \ \frac{99}{70}, \ldots \ , \tag{22}$$

and correspondingly the sequence of best resonant vectors $k \in \mathbf{Z}^2$, namely

$$k = \ (3, -2)\, , \ (7, -5)\, , \ (17, -12)\, , \ (41, -29)\, , \ (99, -70)\, , \ldots \ . \tag{23}$$

The usual methods of classical perturbation theory provide, in such a situation, a poor bound

$$|\Delta I| < C\, e^{-c\sqrt{\omega}} \ . \tag{24}$$

By extending the Landau–Teller heuristic approximation for large λ, we find instead [3] the more precise expression

$$\Delta I \simeq C^* k e^{-\lambda\tau|k\cdot\Omega| - \rho|k|} \ , \tag{25}$$

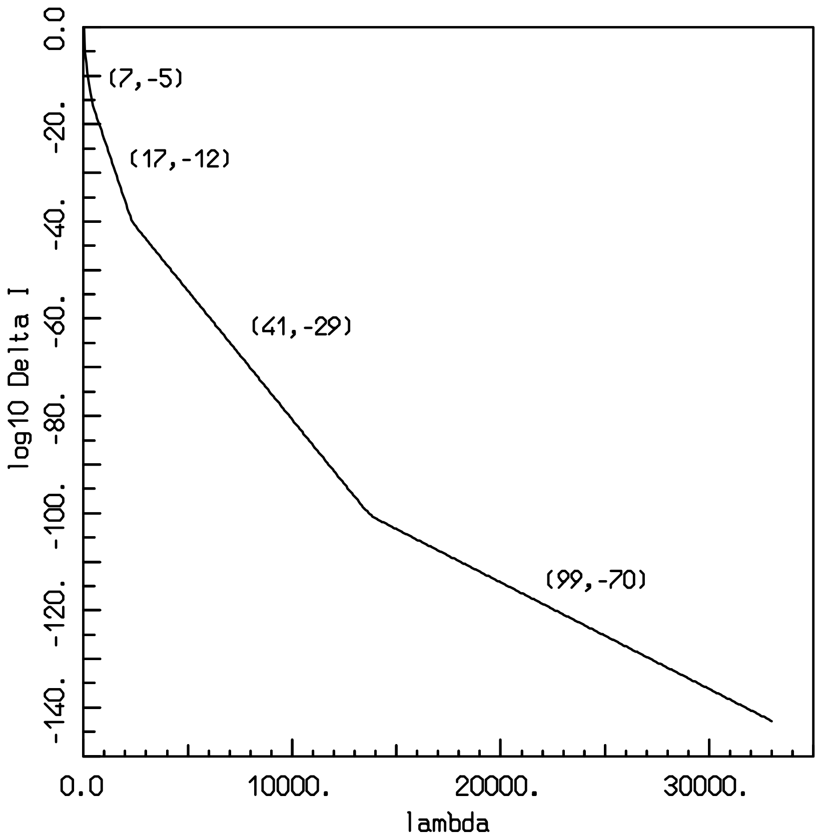

Fig. 6. A numerical plot of (25).

where k is that vector in the sequence (23) minimizing the exponent

$$\sigma = \lambda\tau|k\cdot\Omega| - \rho|k| \ , \tag{26}$$

while C^* is a (well defined, computable) constant.[6] By increasing λ, increasingly larger k enter consideration, and the expected behavior of $\|\Delta I\|$, in a semilog scale, is that represented in Fig. 6. The corresponding k is indicated near each segment of the broken line. Such behavior is consistent with the rough estimate (24),[7] but (25) is much more detailed and precise. Of course

[6] The actual result of the approximation is $\Delta I \simeq C^* \sum_{k\in\mathbf{Z}^2} k e^{-\lambda\tau|k\cdot\Omega|-\rho|k|}$. For large λ, only the integer vectors in the sequence (23) give an appreciable contribution. Moreover, apart from narrow crossover regions where two vectors have comparable size, for each λ just one term in the sum dominates, that minimizing σ. The crossover effect results in some smoothing of the broken line appearing in Fig. 6, and is negligible for large λ.

[7] One can see that in each segment, the broken line is asymptotically tangent to a curve

$$y = a(\tau,\rho)\sqrt{\lambda}\, e^{-\sqrt{c\tau\rho\lambda}} \ , \qquad c = 2+\sqrt{2} \ , \tag{27}$$

with suitable $a(\tau,\rho)$. So the estimate (24), with $\sqrt{\omega}$ in the exponent, is apparently

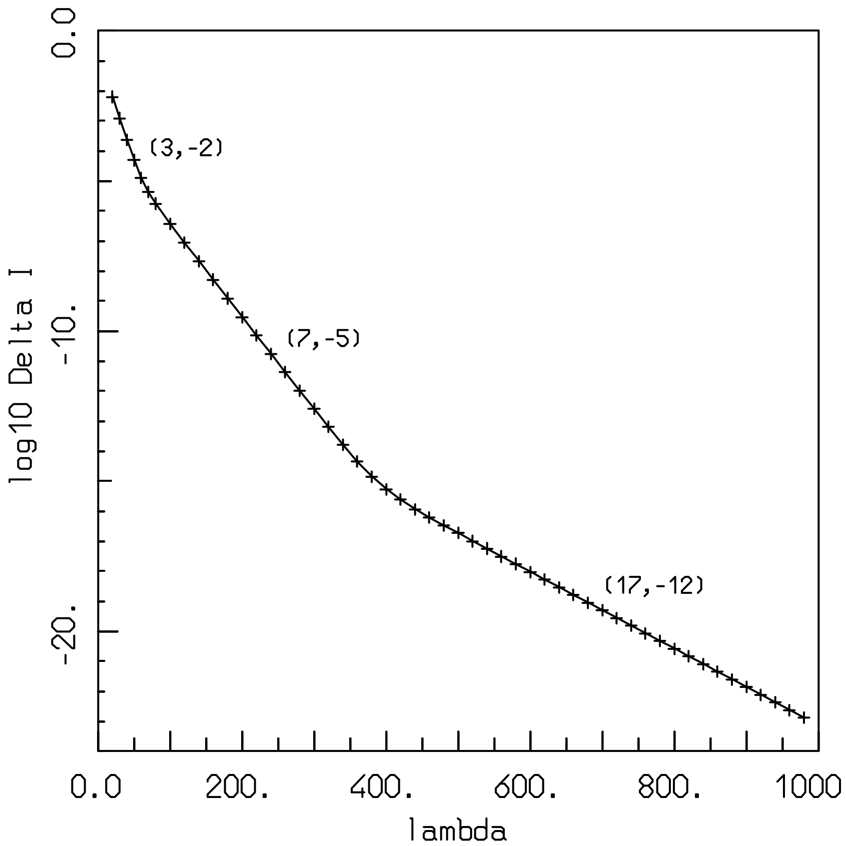

Fig. 7. $\|\Delta I\|$ vs. λ for $\tau = 1$ and $\rho = 1$; crosses represent experimental data, the continuous line is the theoretical expectation; i.e., the broken line of Fig. 6.

this result, being heuristic, needs to be tested. [8]

So, let us now come to the numerical experiments. These were performed, once more, with the leapfrog in quadruple precision, see [3]. Figs. 7 and 8 show the results, for $\tau = 1$ and two choices of ρ; the crosses represent numerical data and the solid line corresponds to the broken line of Fig. 6. The agreement is remarkable (there are no free constants in the theory). We can also make a more precise quantitative comparison between theory and numerical data, by

optimal among simple stretched exponentials.

[8] Well, this is a kind of logical exposition of the results. In reality, we initially tried to check numerically the optimality of the square root law (24). To our great surprise, in place of a continuous curve we found the broken line in Figs. 6 and 7. Searching for a theoretical interpretation of the numerical data, we took into consideration the possibility of extending the Landau–Teller approximation to a two–frequency problem. As a matter of fact, the great precision offered by symplectic integrators was essential for us, for developing the theory.

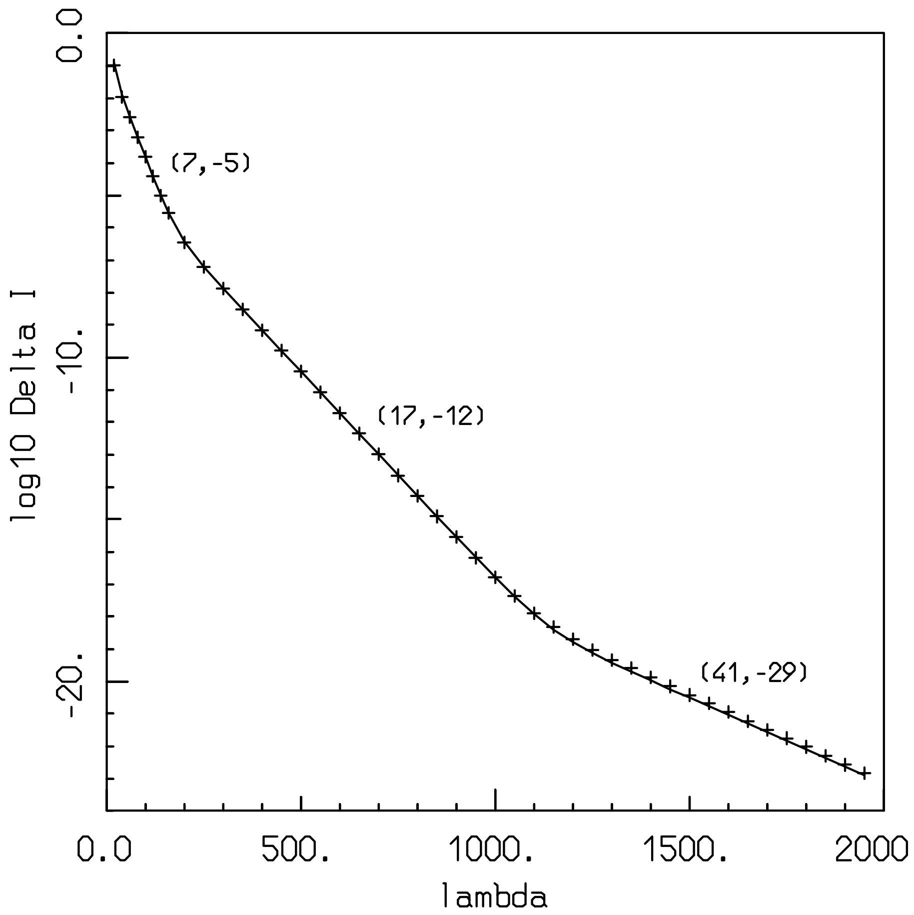

Fig. 8. The same as Fig. 7, for $\tau = 1$ and $\rho = 0.5$.

Table 1.

τ	ρ	k	α	α'	β	β'	γ	γ'
1.0	1.0	(7,-5)	0.0711	0.0709	7.70	7.76	1.400000	1.400003
		(17,-12)	0.02942	0.02943	23.82	23.83	1.416666	1.416666
0.5	1.0	(7,-5)	0.03554	0.03551	7.76	7.78	1.40000	1.40001
		(17,-12)	0.01472	0.01473	23.87	23.88	1.4166666	1.4166666
1.0	0.5	(17,-12)	0.02944	0.02945	9.320	9.325	1.416666	1.416666
		(41,-29)	0.0122	0.0124	28.9	28.4	1.4193793	1.4193793
1.0	0.25	(17,-12)	0.0294	0.0296	2.07	2.10	1.4166	1.4165
		(41,-29)	0.0122	0.0122	11.4	11.1	1.4137931	1.4137931

fitting the different segments in each figure with straight lines $-\alpha_k\lambda-\beta_k$, and comparing the experimental values of α_k and β_k with the theoretical values deduced from (25),

$$\alpha_k=\tau|k\cdot\Omega|\ ,\qquad \beta_k=\rho|k|-\log\|k\|\ . \tag{28}$$

As a further test, we computed the ratio $\Delta I_1/\Delta I_2$ and compared it with the theoretical value, again deduced from (25),

$$\gamma_k=k_1/k_2\ . \tag{29}$$

The results are summarized in Table 1; α,β,γ represent theoretical values and the corresponding primed quantities are the computed values. The agreement is definitely good, and even impressive for γ. In our opinion, it is remarkable that a brute–force, step by step integration of the equations of motion, if performed by a symplectic method, reveals very fine details of the dynamics, and permits exploration of delicate matters such as the arithmetic properties of the frequency vector. That the computed γ gives the best agreement is not surprising. Indeed, as remarked in the previous section, the effect of the symplectic algorithm is to slightly modify the Hamiltonian; this can introduce small changes in α_k and β_k, but certainly not in the ratio $\gamma_k=k_1/k_2$, which is, thus, a particularly "robust" quantity.

The possibility of performing such a fine analysis of the dynamics numerically opens the door to further interesting studies. Indeed, there are situations, such as the case of three independent frequencies, which are presently beyond theoretical analysis; e.g., in lack of the formalism of the continued fraction, the equivalent of sequence (23) is unknown. It is our hope that accurate numerical computations can provide helpful hints.

References

[1] O. Baldan and G. Benettin, Classical "freezing" of fast rotations: Numerical test of the Boltzmann–Jeans conjecture, *J. Stat. Phys.* 62 (1991) 201–219.

[2] G. Benettin, On the Boltzmann conjecture for a classical "freezing" of fast degrees of freedom, Proceedings of the conference: Boltzmann's legacy 150 years after his birth, *Atti Accad. Nazionale dei Lincei* 131 (1997) 89–105.

[3] G. Benettin, A. Carati and F. Fassò, On the conservation of adiabatic invariants for a system of coupled rotators, *Physica D* 104 (1997) 253–268.

[4] G. Benettin, A. Carati and G. Gallavotti, A rigorous implementation of the Jeans-Landau-Teller approximation for adiabatic invariants, *Nonlinearity* 10 (1997) 479–505.

[5] G. Benettin, A. Carati and P. Sempio, On the Landau–Teller approximation for the energy exchanges with fast degrees of freedom, *J. Stat. Phys.* 74 (1993) 175–192.

[6] G. Benettin and F. Fassò, Classical "freezing" of plane rotations: a proof of the Boltzmann–Jeans conjecture, *J. Stat. Phys.* 63 (1991) 737–760.

[7] G. Benettin and A. Giorgilli, On the Hamiltonian interpolation of near to the identity symplectic mappings, with application to symplectic integration algorithms, *J. Stat. Phys.* 74 (1994) 1117–1144.

[8] L. Boltzmann, On certain questions of the theory of gases, *Nature* 51 (1895) 413–415.

[9] L. Boltzmann, *Vorlesungen über Gastheorie,* Barth, Leipzig 1896 (Vol I), 1898 (Vol II) [English translation: *Lectures on Gas Theory,* University of Cal. Press (1966)].

[10] E. Hairer and Ch. Lubich, The life–span backward analysis for numerical integrators, *Numer. Math.* 74 (1977) 441–462.

[11] J. H. Jeans, On the vibrations set up in molecules by collisions, *Phil. Mag.* 6 (1903) 279–286.

[12] L. Landau and E. Teller, Zur Theorie der Schalldispersion, *Physik. Z. Sowjetunion* 10 (1936) 34–43 [English translation: On the theory of sound dispersion, in *Collected Papers of L. D. Landau*, edited by D. Ter Haar, page 147–153 (Pergamon Press, Oxford 1965)].

[13] F. M. Lasagni, Canonical Runge-Kutta methods, *J. Appl. Math. Phys. (ZAMP)* 39 (1988) 952–953.

[14] J. Moser, *Lectures on Hamiltonian Systems,* Mem. American Math. Soc. 81 (1968) 1–60.

[15] A. I. Neishtadt, The separation of motions in systems with rapidly rotating phase, *Prikl. Matem. Mekan.* 48 (1984) 197–204 [*J. Appl. Math. Mech.* 48 (1984) 133–139].

[16] D. Rapp, Complete classical theory of vibrational energy exchange, *Journ. Chem. Phys.* 32 (1960) 735–737.

[17] S. Reich, Backward error analysis for numerical integrators, preprint 1996.

[18] P. Sempio, Scambi di energia tra gradi di libertà caratterizzati da differenti scale temporali: rilassamento all'equilibrio in gas poliatomici e problemi di confinamento magnetico, Ph.D. Thesis (Physics Department, Padova 1993).

A Separating the Fourier components of ΔE

From (6), the Fourier components E_k of ΔE decrease exponentially with $|k|$, so it might be surprising that we can distinguish the components when, for large ω, they differ by many orders of magnitude. As a matter of fact, the exponential decrease is not an obstacle, rather it provides an essential help for separating the components at low cost.

To measure E_k we should compute the integral, hiding all variables but ϕ^o,

$$E_k = \frac{1}{2\pi} \int_0^{2\pi} \Delta E(\phi^o)\, e^{-ik\phi^o} \, \mathrm{d}\phi^o \ . \tag{A.1}$$

In practice, we replace the integral by a finite sum over l equally spaced values $\phi^o = 2\pi j/l$, $0 \le j \le l-1$; i.e., in place of E_k, we compute

$$\widetilde{E}_k = l^{-1} \sum_{j=0}^{l-1} \Delta E(2\pi j/l)\, e^{-2\pi i j/l} \ . \tag{A.2}$$

Now, from the orthogonality relation

$$\frac{1}{l} \sum_{j=0}^{l-1} e^{2\pi i r/l}\, e^{2\pi i s/l} = \begin{cases} 1 & \text{if } r - s = ml \ , \ m \in \mathbf{Z}, \\ 0 & \text{otherwise,} \end{cases} \tag{A.3}$$

we immediately deduce

$$\widetilde{E}_k = E_k + E_{k\pm l} + E_{k\pm 2l} + \cdots \tag{A.4}$$

(the sum extends to both signs in the subscripts). By the exponential decay of the E_k's, in order for all terms $E_{k\pm ml}$, $m > 1$, to be practically negligible compared to E_k, it is sufficient to take

$$l \ge 2k + 1 \ . \tag{A.5}$$

So, three values of ϕ^o *equally spaced* in $(0, 2\pi)$ are sufficient to separate the average E_0 from the much larger fluctuations, while seven values are sufficient to reliably compute each of E_0, E_1, E_2 and E_3. Numerical experiments [1,5] with different values of l, ranging from 7 to “large” values such as 128 or 256, show excellent stability.

B A comparison between leapfrog and Runge–Kutta

Let us come back to Hamiltonian (2), and look what happens if we perform the numerical integration by an algorithm, like the classical fourth order Runge–Kutta (RK4), which is more accurate than leapfrog, but not symplectic. The quantity we shall look at is the relative error δE. Since the algorithm is of order four, the error per step is of order ε^5, so the accumulation of individual errors after a given time (in the lack of compensation mechanisms) is expected to be of order ε^4.

Fig. 9 shows δE plotted against time for two choices of time step. We observe oscillations similar to those of Fig. 3, although less regular. The height of the peaks scales well [9] as ε^4, as expected, and so is definitely smaller, for small time steps, than for leapfrog. But, after the collision the error is not re-absorbed, and the residual error δE provides an effective limit, *much* worse than that of leapfrog, on the possibility of computing small energy exchanges.

Comparing the two parts of Fig. B1, we can observe that by reducing the time step ε, the final value decreases faster than the maximum value of δE. In fact, a quantitative analysis shows that the final value does not scale with ε^4, but with ε^5 (approximately). In other numerical integrations (not reported here), we found a similar phenomenon for more elementary systems, like the one–degree of freedom Hamiltonian

$$H(p,x) = \frac{p^2}{2} + V(x) \ , \tag{B.1}$$

and for lower order (non-symplectic) integrators, like the modified Euler method (ε^4 and ε^5 for RK4 being replaced respectively by ε^2 and ε^3). It is not difficult to understand such a phenomenon in this simpler situation, and we are confident that a similar explanation holds in the more complicated case of RK4 and two degrees of freedom.

The modified Euler method for the Hamiltonian (B.1) reads

$$x' = x + \varepsilon\,(p - \frac{\varepsilon}{2}V'(x)) \ , \qquad p' = p - \varepsilon\, V'(x + \frac{\varepsilon}{2}p) \tag{B.2}$$

(here and below primes on V denote derivatives). The error per step in energy conservation is

$$H(p',x') - H(p,x) = \varepsilon^3\, \eta(p,x) + \mathcal{O}(\varepsilon^4) \ , \qquad \eta(p,x) = \frac{p^3}{24}\, V'''(x) \ . \tag{B.3}$$

After n steps, with $(p',x') = \Psi_\varepsilon(p,x)$,

$$\delta E(n\varepsilon) = \varepsilon^3\, E^{-1} \sum_{j=0}^{n-1} [\eta(\Psi_\varepsilon^j(p,x)) + \mathcal{O}(\varepsilon)]. \tag{B.4}$$

[9] Well, but not as well as with leapfrog: the error in the scaling is about 10%.

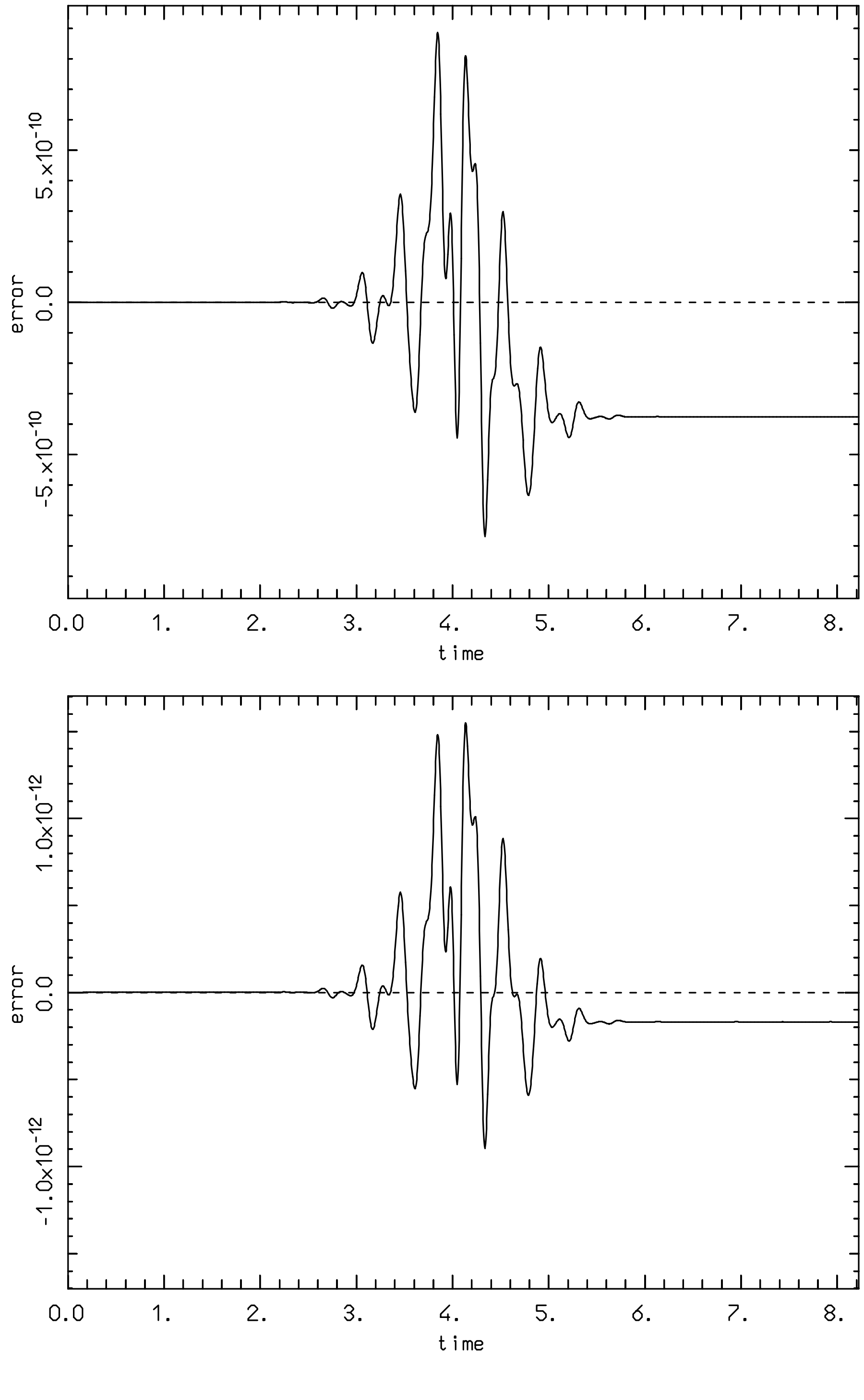

Fig. B.1. The relative error in energy conservation as function of time, for RK4 and two different integration steps: (a) $\varepsilon = 0.01\frac{2\pi}{\omega}$ and (b) $\varepsilon = 0.002\frac{2\pi}{\omega}$. Parameters and data as in Fig. 3.

Since the formula is asymptotically exact, ignoring round–off, we deduce

$$\Psi_\varepsilon^n(p,x) = \Phi_{n\varepsilon}^H(p,x) + \mathcal{O}(\varepsilon) \tag{B.5}$$

uniformly in n, and

$$\begin{aligned} \delta E(n\varepsilon) &= \varepsilon^3\, E^{-1} \sum_{j=0}^{n} [\eta(\Phi_{j\varepsilon}^H(p,x)) + \mathcal{O}(\varepsilon)] \\ &= \varepsilon^2\, E^{-1} \int_0^t \eta(\Phi_t^H(p,x))\ \mathrm{dt} + \mathcal{O}(\varepsilon^3) \end{aligned} \tag{B.6}$$

where $t = n\varepsilon$. Since, as is immediately checked,

$$\eta(p,x) = \frac{\mathrm{d}}{\mathrm{dt}}\,[p^2 V''(x) - (V'(x))^2], \tag{B.7}$$

it follows that, if the initial datum is taken long before the collision so that V' and V'' both vanish initially, then

$$\delta E(t) = \frac{\varepsilon^2}{24\,E}[p^2(t)V''(x(t)) - (V'(x(t))^2] + \mathcal{O}(\varepsilon^3). \tag{B.8}$$

The order ε^2 term corresponds to the oscillations of δE during the collision, while the order ε^3 term gives the final value.